The conditional inhibition of gene expression in cultured *Drosophila* cells by antisense RNA

Thomas A.Bunch+ and Lawrence S.B.Goldstein*

Department of Cellular and Developmental Biology, Harvard University, Cambridge, MA 02138, USA

Received August 8, 1989; Revised and Accepted November 2, 1989

ABSTRACT

Genes producing antisense RNA are becoming important tools for the selective inhibition of gene expression. Experiments in different biological systems, targeting different mRNAs have yielded diverse results with respect to the success of the technique and its mechanism of action. We have examined the potential of three antisense genes, whose transcription is driven by a *Drosophila* metallothionein promoter, to inhibit the expression of alcohol dehydrogenase (ADH) or a microtubule associated protein (205K MAP) in cultured *Drosophila* cells. Expression of ADH was significantly reduced upon induction of the anti-ADH genes. The ADH mRNA does not appear to be destabilized by the presence of antisense RNA but rather exists at similar levels in hybrid form. Hybrids are detected with both spliced and unspliced ADH RNA. In contrast to these results, antisense genes producing antisense RNA in great excess to 205K MAP mRNA, which is itself far less abundant than the ADH mRNA, failed to show any inhibition of 205K MAP expression.

INTRODUCTION

In recent years, antisense genes, which produce RNAs that are complementary to mRNA, have been engineered *in vitro*, transfected into cells and shown to be effective in inhibiting gene expression in several biological systems (1−12). Despite the success of this technique in diverse organisms, no clear picture has emerged concerning various aspects of antisense inhibition. Thus, in some systems inhibition requires that the antisense RNA be present at levels greater than 40 fold over mRNA (5,6,13), while in others only a 1−5 fold excess is needed (2,6,9,11,14,15). In one case hybrids of mRNA and antisense RNA are found in the nucleus (7) and in others hybrids have been detected in the cytoplasm (14). In still others the mRNA appears to be destabilized, indicating that the cell has mechanisms for selectively degrading the hybrid RNAs or that lack of translation, due to the hybrid formation, reduces the stability of the mRNA (2,8,10,16,17). In one system it appears that the hybrid region may be stable while the rest of the mRNA is targeted for degradation (14). Finally, some cells appear to have an activity that unwinds the hybrids and prevents inhibition of gene expression (18,19). The regions of the mRNAs that have been targeted for hybrid formation also have given diverse results. Successes and failures have been noted for antisense experiments that utilize antisense RNA complementary to the 5′ or 3′ untranslated sequences, the coding regions, and intron/exon boundaries in the mRNA (7,8,13,21,22).

This diversity of results indicates that there may be differences in the cellular responses to the presence of RNAs that can form hybrids. These differences may depend on the biological system that is being used and the mRNA that is being targeted. To gain a clearer understanding of the mechanisms of antisense inhibition of gene expression, careful analysis

of both successes and failures of the antisense technique in several systems and for a variety of genes is important. This enhanced understanding will be useful in understanding the fate of double stranded RNA in cells as well as in designing future antisense experiments.

In this report we present our findings on attempts to inhibit the expression of alcohol dehydrogenase (ADH), which is expressed from exogenously added genes, and a microtubule associated protein (205K MAP) (23), which is expressed from an endogenous gene, in cultured *Drosophila melanogaster* cells. To achieve this we have constructed antisense genes whose transcription is regulated by the metallothionein promoter. The production of antisense RNA can therefore be regulated by varying the media conditions. Inhibition of ADH expression was achieved but we were unsuccessful in our attempts to inhibit 205K MAP expression. We examine the amount of inhibition and characterize the RNAs, including antisense RNA, mRNA, and hybrids, that are present during these experiments. These experiments indicate that in the case of ADH, hybrids do form *in vivo*, and these hybrids are stable, not targeted for degradation, and prevent translation of ADH mRNA.

MATERIALS AND METHODS

Drosophila Cell Culture and Transformation

S2/M3 cells are Schneider's line 2 cells (24) adapted for growth in M3 medium (25). S2/M3 cells were grown in M3 medium supplemented with 12.5% fetal calf serum (FCS), which has been heat inactivated at 60°C for 30 minutes. Transformed cells were grown in M3 medium + 12.5% FCS + 2×10^{-7} M methotrexate (methotrexate stock solution is 4×10^{-4} M in 50 mM sodium carbonate). Cells were transformed using the calcium phosphate co-precipitate method (26) as previously described (27). Selection of transformants was achieved by culturing the transformed cells in methotrexate. The plasmid pHGCO was included in the transfections and contains the bacterial dihydrofolate reductase gene which confers resistance to methotrexate in transformed cells (28). Soft-agar cloning of cell lines has been previously described (29). The DNA transfected into the cells was a 5:1:14 ratio of plasmids pEIP-ADH:pAnti-ADH:pHGCO (described below) in clone ADHa1, 15:1:4 in clone ADHa2 and 50:1:150 in ADHa3. For clones ADHc1 and ADHc2 the ratio was 5:1:14 and 15:1:4 of pEIP-ADH:p5'sense-ADH:pHGCO (described below). Clones MAPa5 and MAPa6 were derived from S2/M3 cells transformed with a 1:1 ratio of plasmids pAnti-cMAP:pHGCO (described below) and clones MAPa7 and MAPa8 were transformed with a 1:10 ratio. Clones MAPa1, MAPa2, MAPa3 and MAPa4 were derived from S2/M3 cells transformed with 1:1, 1:1, 1:10 and 1:10 ratios of plasmids pAnti-5'MAP:pHGCO (described below). Following completion of this work the clone ADHa2 was lost.

Induction of transcription from the metallothionein promoter was achieved, as previously described (27), by adding $CuSO_4$ to 0.3 mM to the growth medium of the cells.

Metabolic Labelling of Cultured Cells

5×10^6 cells were collected by centrifugation in an IEC (International Equipment Co.) clinical centrifuge at setting 6 [approximate RCF (relative centrifugal force) — 1100] for 20 seconds. The cells were washed 3–4 times in 4 ml of methionine-free medium, resuspended in 0.5 ml of methionine-free medium, and placed in one well of a 24 well tissue culture plate. 75 μCi (1000 Ci/mmole) of Trans^{35} S-label (ICN #51006) were added. Cells were collected by centrifugation after 6 hours of labelling. Preliminary

experiments demonstrated that labelling under these conditions results in the linear incorporation of TCA (trichloroacetic acid) precipitatable counts for 10 hours.

Immunoprecipitation of 205K MAP and Cytoplasmic Myosin

Cell pellets were resuspended and lysed at a concentration of 2.5×10^7 cells/ml in RIPA [10 mM Tris-HCl (pH 7.4); 150 mM NaCl; 1% Triton x-100; 1% deoxycholic acid; 0.1% SDS; 1 μg/ml leupeptin, pepstatin and aprotinin; 2 μg/ml TAME (N alpha-p-Tosyl-L-arginine Methyl Ester); 1 mM PMSF (phenylmethylsulfonyl fluoride); and 2 mM DTT (dithiothreitol)]. Cell debris was removed by centrifugation, at 4°C, in a microfuge at top speed for 2 minutes. Neither 205K MAP nor cytoplasmic myosin is pelleted in this step. Pansorbin (Calbiochem #507858) was equilibrated with RIPA and brought to a concentration of 10% (w/v). IgG from serum from rabbit 886 (Gorman and Goldstein, unpublished data), that contains antibodies that bind to the carboxyl terminus of 205K MAP, or from rabbit 656 (30), that contains antibodies against *Drosophila* cytoplasmic myosin heavy chain, was bound to the Pansorbin by incubating 40 μl of serum with 200 μl of the Pansorbin in RIPA. This incubation was for 30−60 minutes on ice with occasional mixing. The Pansorbin with IgG bound was centrifuged briefly (as little as necessary to pellet the Pansorbin) and the supernatant removed. The Pansorbin + IgG was washed 2×, by vortexing and pelleting, with 300 μl of RIPA and finally resuspended in 200 μl of RIPA. 40 μl of Pansorbin + IgG was mixed with 50 μl of cell extract and incubated for 60 minutes on ice. The Pansorbin + IgG + 205K MAP (or myosin) was collected by centrifugation. The supernatant was removed and the pellet was washed 4× with 300 μl of RIPA*. Finally the pellet was resuspended in 25 μl of 1.5× Laemmli sample buffer (31) and boiled for 5−10 minutes to remove the proteins from the Pansorbin. The Pansorbin was pelleted by centrifugation and the supernatant was collected and 10 μl were loaded onto a SDS PAGE gel (31). Analysis of precipitated and unprecipitated 205K MAP and myosin by immunoblots demonstrated that this procedure results in the precipitation of greater than 80% of the 205K MAP or myosin in these cells.

Plasmid and Probe Constructions

pEIP-ADH contains the EIP 28/29 promoter (32) that begins 656 bases 5′ from the cap site and ends 11 bases downstream of the cap site. This has been cloned into the *Pst*I site of plasmid pUC8 (L. Cherbas and E. Lander, personal communication). This constitutive promoter is followed by 11 bases of polylinker from pUC8 and then the structural gene for the *Drosophila melanogaster* alcohol dehydrogenase gene, beginning 31 bases 3′ of the larval cap site and extending 1.2 kb 3′ to the polyadenylation site. The Adh fragment was taken from pSAC1, described in Goldberg, 1980 (33).

The plasmids pAnti-ADH and p5′sense-ADH (see figure 1c and 1d) were obtained by cloning the *Bam*HI fragment from pEIP-ADH in either the reverse or the correct orientation, relative to the promoter, into the *Bam*HI site of the vector pRmHa-1. The ADH sequences include 40 bases of the 5′ untranslated leader sequence, the first exon, the first intron and 315 bases of the second exon. The cap site is not covered by the antisense RNA produced from pAnti-ADH plasmid. The expression vector pRmHa-1 contains the promoter and cap site from a *Drosophila melanogaster* metallothionein (MT) gene, polylinker sequences and the polyadenylation signal from the ADH gene (27).

To synthesize protection fragments, shown in figure 1b, *in vitro* the *Bcl*I fragment from pEIP-ADH was cloned in both orientations into the transcription vector pGEM4 (Promega Biotech), which contains the T7 promoter. By digesting the resulting plasmids with *Eco*RI

and transcribing them from the T7 promoter we obtain the protection fragments SP1 and AP1. Digestion of the plasmid used to synthesize SP1 with *Bam*HI followed by transcription from the T7 promoter gives SP2 while digestion of the other plasmid with *Bam*HI followed by transcription gives the protection fragment AP2.

The *Bam*HI fragment, DS1, shown in figure 1b was isolated and radiolabelled by the random hexanucleotide primed synthesis method (34).

pAnti-cMAP was constructed by cloning a 2.4 kb *Eco*RI fragment from a cDNA for 205K MAP (23) into the *Eco*RI site of pUC18 (35). This plasmid was then digested with *Bam*HI, which cleaves the 205K MAP DNA 400 bases 3′ to the *Eco*RI site (E′ in figure 8) and pUC18 in its polylinker 25 basepairs 3′ of the second *Eco*RI site (E″ in figure 8). This *Bam*HI fragment was cloned in reverse orientation with respect to promoters, into the expression vector pRmHa-1. This plasmid has been previously described and was called pMMAP-1 (27).

pAnti5′-MAP was constructed by cloning the *Sal*I fragment from a DNA clone into the expression vector pRmHa-1 in reverse orientation with respect to promoters. The 5′ *Sal*I site (S' in figure 8 is derived from the polylinker sequences that the cDNA was cloned into.

Plasmid pSkrh49 (not shown) is based on the transcription vector Bluescript-SK (Stratagene). Into the *Eco*RI and *Hind*III sites of its polylinker was cloned the *Eco*RI-*Hind*III fragment of the 49kd ribosomal ribosomal protein (RP49) gene [from subclone H4 (36)]. By digesting this plasmid with *Eco*RI and transcribing from the T7 promoter we obtain a protection RNA that will hybridize to the RP49 mRNA in RNase protection experiments. As this plasmid, pSKrh49, is derived from genomic sequences that contain an intron, digestion of the hybrid with RNase followed by probing of the protected RNAs with a double stranded probe detects 3 protected RNA fragments. One protected fragment is 410 nucleotides and is derived from the mRNA and the other two, 310 and 103 nucleotides, are derived from the protection RNA that is cleaved in the looped out intron of the hybrid. Shown in figures 3 and 4 are just the two larger bands but the 103 nucleotide band is also present in our autoradiographs.

Nucleic Acid Preparation and Northern Analysis of RNA

Total nucleic acids were extracted from cell pellets by a protease K, phenol/chloroform extraction procedure (27). Poly (A+) RNA was selected with oligo (dT)-cellulose (microcrystalline) [New England BioLabs # 1403] as suggested by the supplier. RNAs were electrophoresed on formaldehyde gels (37) and blotted onto GeneScreen nylon filters as suggested by the manufacturers. Instead of baking the filters, we have used the U.V. crosslinking technique of Church and Gilbert (38) to crosslink the RNA to the filter. Prehybridization (2−60 minutes) and hybridization (14−18 hours) were carried out at 42°C in 50% formamide, 5×SSC, 50 mM sodium phosphate, 250 μg/ml sheared denatured calf-thymus DNA, 0.5% SDS, 1× Denhardt's (39). Radiolabelled probes were added during the hybridization step and were prepared by the random hexanucleotide primed synthesis method (34). Radiolabelled RNAs were also used as probes. After hybridization, the filters were washed in 2× SSC, 0.5% SDS (four 15 minute washes at 23−37°C), and 0.1× SSC, 0.5% SDS (two 15 minute washes at 50°C). When radiolabelled RNAs were used the hybridization and wash conditions were increased to 65°C.

RNase Protections

RNase protection experiments were done as described in reference (21) using *in vitro* synthesized protection RNAs. These protection RNAs were synthesized using T7 polymerase and the T7 promoters of the cloning vectors pGEM4 (Promega Biotech) or

the Bluescript vectors (Stratagene) into which had been cloned portions of the ADH or 205K MAP gene. RNase T1 was used at a concentration of 1 μg/ml and digestions were for 30 minutes at 37°C. RNase A was not used as it cleaved the ADH mRNA:SP1 protection fragment (see figure 1 for a description of RNAs) in an AT rich region of the hybrid. Since RNase T1 was the only RNase used and it cleaves the single stranded RNA following only G residues the sizes of the protected RNAs are approximately those that we expect but not exactly. These sizes vary by as much as 40 nucleotides due to the lack of G residues that are not involved in any secondary structure. This point is most clearly seen in figure 3b. In figure 3b we expect one protected fragment from SP1 protecting ADH mRNA (arrow 2) and one copper-inducible protected fragment for the protection of the ADH-5'sense RNA with SP1 (arrow 4, lanes 3,4,6 and 7). However, an additional band (arrow 3) is also detected. The protection RNA SP1 is properly digested to give the smaller protection fragment (arrow 4). This was demonstrated by using radiolabelled SP1. The other band (arrow 3), then, is derived from the ADH 5'-sense RNA not being completely digested, perhaps due to secondary structure protecting the G residues that follow the hybrid.

Experiments that examine the presence of hybrids *in vivo* were done by resuspending the RNA from an ethanol precipitate of total RNA directly into RNase buffer containing RNase, without a hybridization step.

Most of the RNase experiments were done with protection fragments that were not radiolabelled. In this case the protected RNAs were visualized by probing electroblots with radiolabelled RNA or DNA probes. The RNAs were electrophoresed on denaturing urea polyacrylamide gels and then electroblotted onto Nytran nylon membrane (Schleicher and Schuell #41-01870) as suggested by the manufacturer. The RNA was UV crosslinked and probed using the same conditions that are described in the RNA analysis section.

Scanning Densitometry

Filters or dried gels containing radiolabelled RNA or DNA were exposed to preflashed Kodak X-OMAT AR diagnostic film. Intensifying screens (Dupont-Cronex Lightning-Plus EG) were used and exposures were done at −70°C. The indicated bands of the autoradiographs were scanned using a Hoefer Scientific Instruments GS 300 Transmittance/Reflectance Scanning Densitometer. Background CPM were subtracted and then the RP49 signal intensities for each experiment were used to correct for loading or manipulation errors. Following this correction, the signal intensity of the most intense band in each film (for each experiment, or figure there were two films as each was done in duplicate) was arbitrarily set at 100 and the others were normalized to this. The results from the duplicate experiments were averaged and presented in Table 1. For the quantitation of ADH mRNA and anti-ADH RNA for figure 3a, and columns 1 and 2 of Table 1, multiple exposures for different times were examined and the numbers obtained are within the linear range of the film and are therefore an accurate representation of RNA levels. This was not done for the other quantitations and therefore the other numbers in Table 1 are close to, but not absolutely, indicative of the RNA levels. By comparison with the multiple exposures that were done for figure 3a, we can conclude that the only numbers in Table 1 that are more than a factor of 2 off are the very faint bands with values lower than 5.

ADH Assays

ADH activity was determined by a modification of the assay described in Sofer and Ursprung (40). Frozen cell pellets (−70°C) containing $1-8\times10^7$ cells were resuspended in 200 μl of 1% Triton X-100, 50 mM Tris·PO_4 (pH 8.6). The cells were lysed by vortexing and cellular debris was removed by spinning the extract in a microfuge at top speed for 2 minutes, at 4°C. The supernatant was removed and assayed for protein concentration

[using the BioRad Laboratories assay mix # 500-0006 and BSA as a standard] and ADH activity. To measure ADH activity 10−30 μl of extract was mixed with 50 mM Tris·PO_4 (pH 8.6), 5 mg/ml NAD [Boehringer Mannheim # 127 981], 2% sec-butanol. OD_{340} was measured periodically over a period of 2−4 minutes to obtain the change in OD_{340} per minute. Only measurements that fell within the linear range of the curve were used. By normalizing for protein concentration the ADH specific activity was obtained and is expressed as OD_{340}/min·mg protein.

RESULTS

Anti-ADH Cell Lines

We are interested in using stably integrated antisense genes to inhibit the expression of various genes in cultured *Drosophila melanogaster* cells. As the inhibition of an essential gene would be toxic to the cell we reason, as others have, that the promoter used to drive transcription of the antisense RNA in such experiments should be regulatable. This allows us to transfect the cells under conditions where transcription from the antisense genes is low and then induce the antisense genes and look for inhibition and possibly a phenotype. Toward this end we have previously characterized a metallothionein promoter from *Drosophila melanogaster* and have constructed expression vectors based on this promoter that can be induced by adding copper to the medium (27).

In order to test whether antisense RNA inducibly produced from this vector can inhibit the expression of a *Drosophila* enzyme, we have cotransfected cultured *Drosophila melanogaster* cells (cell line S2/M3) with a plasmid that contains the ADH structural gene whose transcription is promoted by a constitutive promoter. In addition, we cotransfected these cells with the vector containing the metallothionein promoter into which has been cloned about half of the ADH gene in reverse orientation, and the plasmid pHGCO. The plasmid pHGCO (not shown) contains the bacterial DHFR gene and allows us to select transformants in methotrexate containing medium (28).

The ADH promoter is not active in the cultured S2/M3 cell line and stable transformation of these cells with additional copies of the ADH gene bearing its own promoter does not result in ADH expression (29). Therefore we have used a chimeric gene that contains promoter sequences from the EIP28/29 gene followed by the ADH gene. This chimeric gene EIP-ADH has been previously shown to produce a constitutive level of ADH when transfected into S2/M3 cells (data not shown). This plasmid is diagrammed in figure 1a.

Figure 1c shows the plasmid pAnti-ADH. Transcription of anti-ADH RNA is promoted by the metallothionein promoter. To enhance the stability of the antisense RNA there is also a polyadenylation signal in the vector which was derived from the ADH gene.

As a control we have constructed the plasmid p5′sense-ADH, which is exactly the same as pAnti-ADH except the ADH sequences are in the sense orientation (figure 1d). Transfection of cells with this 5′sense-ADH gene alone does not result in ADH activity as the ADH structural gene has been truncated (not shown). Control cells were transformed with pEIP-ADH, p5′sense-ADH and PHGCO.

Cells were transfected with different ratios of pEIP-ADH and either pAnti-ADH or p5′sense-ADH. Populations of transfected cells were selected in methotrexate containing media and assayed for ADH activity either before or after adding 0.3 mM $CuSO_4$ to the medium. Those populations containing pAnti-ADH, but not the controls, showed an inducible inhibition of ADH activity (not shown). To examine this in more detail we obtained clones from the populations that contain EIP-ADH genes and either anti-ADH genes (clones

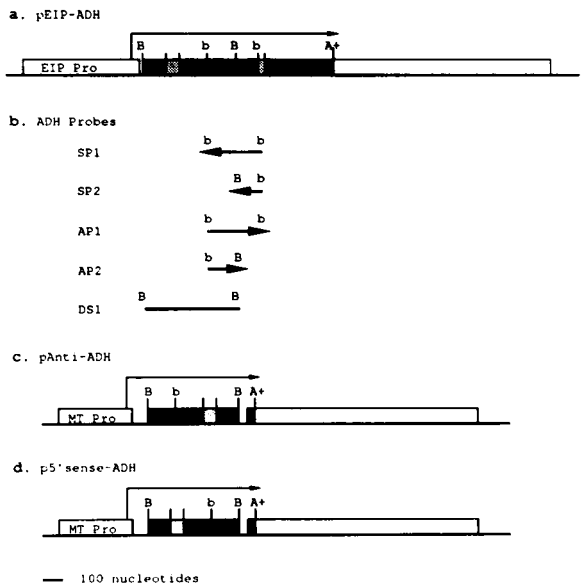

Figure 1. ADH RNA Producing Plasmids and Probes. *a.* Plasmid pEIP-ADH contains the promoter from the EIP 28/29 gene (32). It is not inducible with ecdysone and serves as a constitutive promoter. This has been placed 5′ to the *Drosophila* ADH gene at position +31 (+1 representing the transcriptional start site) of the larval transcript. The entire coding region for ADH is included as well as the two introns, polyadenylation signal and an additional 1.2 kb of sequence 3′ to the polyadenylation signal. *b.* Probes SP1 (sense protection 1), SP2, AP1 (antisense protection 1), AP2 and DS1 (double stranded probe 1) are shown beneath the regions of the ADH gene that they were derived from. SP1 and AP1 probes are synthesized from the pGEM4 vector which contains the *Bcl*I fragment from ADH cloned into the *Bam*HI site in two different orientations. These were linearized with *Eco*RI and the transcription reaction using T7 polymerase produced the two respective probes. SP probes hybridize to mRNA while the AP probes hybridize to antisense RNA. Probe SP2 utilized the same pGEM4 based plasmid that generated SP1 but in this case it was linearized with *Bam*HI. The same is true for probe AP2 except that it was derived from the plasmid that synthesizes AP1 which has been digested with *Bam*HI. The *Bam*HI-*Bam*HI DNA fragment DS1 was isolated and radiolabelled DNA produced by the random hexanucleotide primed synthesis method. This provided a probe that detects both strands of protected RNA. *c.* Plasmid pAnti-ADH was constructed by cloning the *Bam*HI-*Bam*HI fragment from the ADH gene into the transcription vector pRmHa-1 (27) in reverse orientation relative to its promoter. Transcription in this plasmid is driven by the inducible metallothionein promoter. *d.* Plasmid p 5′sense-ADH is identical to pAnti-ADH except that the *Bam*HI ADH fragment has been cloned into the vector pRmHa-1 in the sense orientation.

Open boxes, labelled EIP Pro or MT PRO represent the promoter regions of the genes; closed boxes regions from the ADH gene; shaded boxes are introns in the ADH gene and heavy lines at either end of the plasmid are either pUC8 sequences (in pEIP-ADH) or pUC18 sequences (in pAnti-ADH and p 5′sense-ADH) which are not drawn to scale. The open boxes that are not labelled represent genomic sequences that are 3′ to the ADH polyadenylation signal. Abbreviations are EIP, ecdysone inducible polypeptide; B, *Bam*HI; b, *Bcl*I; MT metallothionein; Pro, promoter; A+, polyadenylation signal.

ADHa1, ADHa2 and ADHa3) or 5′sense-ADH genes (clones ADHc1 and ADHc2) and we examine them in detail below. Southern analysis of genomic DNA (not shown) from these clones has shown that there are approximately 600, 3500, 2000, 2000, and 2000 copies of the EIP-ADH gene present in ADHa1, ADHa2, ADHa3, ADHc1, and ADHc2 respectively. There are approximately 30, 300, and 25 copies of the Anti-ADH genes in clones ADHa1, ADHa2, and ADHa3. Clones ADHc1 and ADHc2 contain approximately

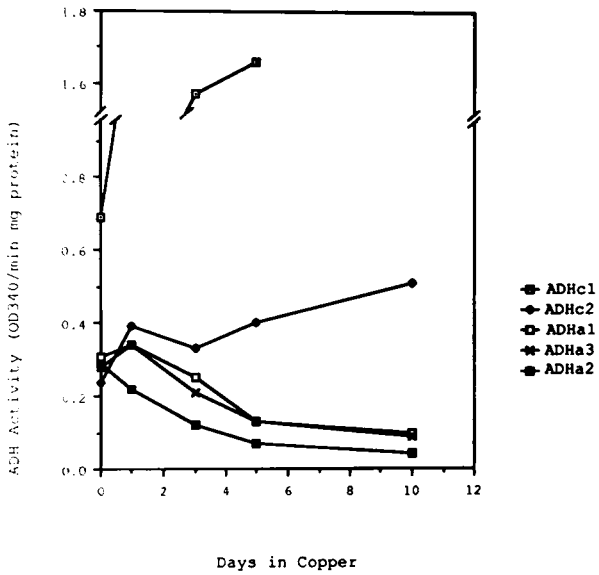

Figure 2. ADH Activity Levels. The ADH activity levels are expressed in units of OD340/min. mg. protein and were assayed in control clones ADHc1 and ADHc2 and the clones that contain anti-ADH genes—ADHa1, ADHa3 and ADHa2. The levels were assayed in cells grown in the absence of $CuSO_4$ or in the presence of 0.3 mM $CuSO_4$ for 1, 3, 5 or 10 days. The points represent the average of duplicate experiments done in parallel. The background levels of activity in untransformed cells varies between 0.02 and 0.05.

50 and 85 copies of the 5'sense-ADH genes respectively. These genes are present in large tandem arrays of the plasmids bearing them that are formed and integrated into the chromosome (28−29). Also present in these arrays are copies of the plasmid pHGCO.

Analysis of ADH Activity

Figure 2 demonstrates that the anti-ADH genes are capable of inhibiting the expression of ADH activity. ADH activity was measured at time point 0, under conditions of no induction of anti-ADH or 5'-sense ADH RNA, or following 1, 3, 5 or 10 days of growth in 0.3 mM $CuSO_4$. Untransformed S2/M3 cells give activities of 0.02−0.05 OD_{340}/min·mg protein. If we subtract the lowest background of 0.02 OD_{340}/min·mg protein from the ADH activities shown, then clones ADHa1, ADHa2 and ADHa3 show inhibitions of 70%, 94% and 75%, respectively. These numbers then represent a minimum estimate of the inhibition for each of the three clones. The control clones ADHc1 and ADHc2 actually show an increase in ADH activity of 2−3 fold. We do not understand the reason for this increase but we do note a 1.5−2 fold increase in ADH activity in cells which contain only EIP-ADH (not shown). This increase is somewhat variable from experiment to experiment while the inhibition is quite constant.

Examination of ADH RNAs

To better understand the mechanisms and requirements of antisense inhibition, we have analyzed the levels of the various ADH RNAs — mRNA, antisense RNA or 5'sense-RNA and hybrid RNA — present in the cells at different times before and during inhibition. We have used RNase protection experiments to study these RNAs. Individual RNAs were examined by hybridizing total RNA extracted from the cells with *in vitro* synthesized RNAs

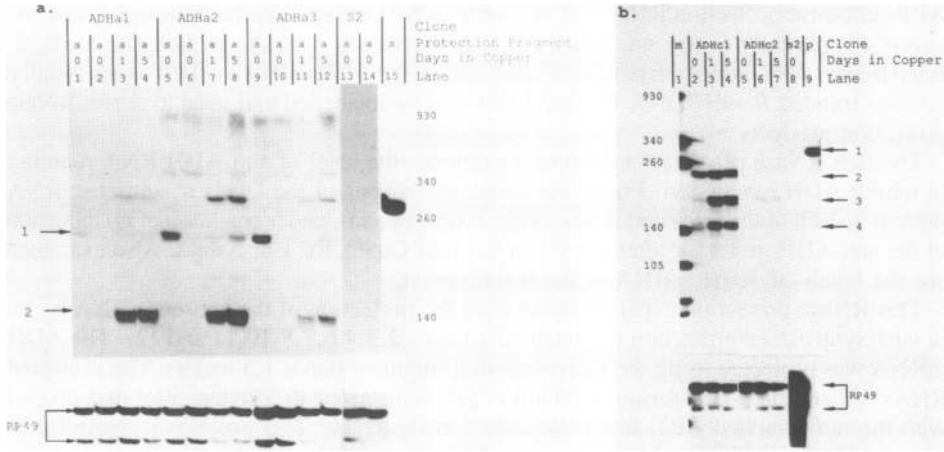

Figure 3. Examination of ADH RNA Levels. *a.* Total RNA was isolated from the clones ADHa1 (lanes 1−4), ADHa2 (lanes 5−8), ADHa3 (lanes 9−12), and S2/M3 cells (lanes 13 and 14), which had not been grown in the presence of 0.3 mM $CuSO_4$ (day 0) or had been grown in the presence of copper for 1 or 5 days. This RNA was hybridized with the protection fragment AP1 (see figure 1), which hybridizes to the anti-ADH RNA (lanes labelled a), or with the protection fragment SP1, which hybridizes to the ADH mRNA (lanes labelled s). A dilution of the two protection fragments that have not been treated with RNase, is shown in lanes 15 and 16. Following RNase treatment the protected RNAs were electrophoresed, blotted to nylon filters and these were probed with radiolabelled probe DS1 (see figure 1). Arrow 1 indicates the expected protection RNA from protection of ADH mRNA (lanes 1, 5 and 9). Arrows 2 indicates the protected RNA obtained from protection of anti-ADH RNA. The other bands result from hybrids formed between ADH mRNA and anti ADH RNA or from complex tri-molecular structures formed between these two RNAs and the added protection fragments. Also included in this protection experiment was an RNA that protects RP49 RNA. The results of this protection are shown and are used to correct for loading errors. *b.* RNA from the control clones ADHc1 and ADHc2, which had not been induced (day 0) or had been grown in the presence of 0.3 mM CuSO4 for 1 or 5 days, and untransformed S2/M3 cells was hybridized with the protection RNA SP1. The RNAs were then treated with RNase, and the protected RNAs were electrophoresed, blotted to nylon filters and these were probed with radiolabelled probe DS1. Arrow 1 indicates undigested protection RNA SP1 which was run in lane 9. Arrow 2 indicates the expected protected RNA from protection of ADH mRNA. Arrows 3 and 4 point to the protected RNA resulting from the hybridization of SP1 with the 5′sense-ADH RNA (explained in more detail in the RNase Protection section of the Materials and Methods). Protection of RP49 mRNA is also shown and was used to correct for loading errors. The intense RP49 signal in lane 8 shows that the S2/M3 sample was extremely overloaded and still shows no protection of SP1.

The abbreviations m,p,and s2 stand for molecular weight markers, probe and S2/M3 cells respectively.

(protection RNAs) that should hybridize to various regions of the ADH mRNA, anti-ADH RNA, and 5′sense RNA. Preliminary experiments were done to demonstrate that in all of the RNase protection experiments we used a vast probe excess. Following hybridization the samples were digested with RNase T1. The hybrid regions are protected from digested and are electrophoresed on denaturing gels, electroblotted to nylon filters and probed with radiolabelled RNA or DNA probes. To examine hybrids that may be formed in the cells, we have extracted total RNA and then treated it directly with RNase T1 without a prior hybridization step.

Figure 1b shows the origins of the protection RNAs that are used in these protection experiments. SP1 (sense protection RNA 1) extends from the 3′ *BclI* site and extends to the 5′ *BclI* site. This hybridizes to the ADH mRNA and partially to the 5′sense RNA.

AP1 (antisense protection RNA 1) is the same as SP1 except it is the opposite strand and hybridizes partially to the anti-ADH RNA. SP2 extends from the 3′ *Bcl*I site to the 3′ *Bam*HI site. AP2 extends from the 5′ *Bcl*I site to the 3′ *Bam*HI site. DS1 is an isolated double-stranded *Bam*HI DNA fragment that was radiolabelled and used to detect RNase protection products.

The first RNase protection experiment examines the level of anti-ADH RNA required to inhibit ADH expression. Figure 3a shows an analysis of the levels of antisense RNA present in each of the three anti ADH clones at time point 0, under condition of no induction of the anti-ADH genes, or after growth in 0.3 mM $CuSO_4$ for 1 or 5 days. Also examined are the levels of ADH mRNA at the 0 time point.

This RNase protection experiment involves the protection of the antisense RNA by an *in vitro* synthesized protection fragment AP1 (lanes 2,3,4,6,7,8,10,11 and 12). The ADH mRNA was protected using the SP1 protection fragment (lanes 1,5 and 9). The protected RNAs are run on a denaturing acrylamide gel, transferred to a nylon filter and probed with the radiolabelled AP2, that is described in figure 1d. This probe will hybridize to one strand of the protected hybrids formed between ADH mRNA and SP1 and to one strand of the hybrid formed between anti-ADH RNA and AP1. The predominant inducible band, indicated by arrow 2, is derived from the protection of the antisense RNA by AP1. It is clear that there is a large induction of antisense RNA in these cells. The protected RNA in lanes 1, 5, and 9 (indicated by arrow 1) is derived from protection of ADH mRNA by SP1. The other bands are due to protection of RNAs in tri-molecular structures formed between the ADH mRNA, the anti-ADH RNA and the protection fragment. This was shown to be the case by using strand-specific probes to various regions of the ADH RNA (not shown).

To obtain a more quantitative understanding of the levels of antisense RNA required to inhibit ADH mRNA translation we have examined the levels of the bands indicated by arrows 1 and 2 in figure 3a by scanning densitometry. To correct for any loading or manipulation errors a control RNA encoding the 49 Kd ribosomal protein (RP49) was also examined in these experiments. The results of protection of RP49 are shown below the ADH protection results. Following correction for loading errors the results from two duplicate experiments were normalized and averaged and are presented in Table 1. If we assume that ADH mRNA levels do not change at days 1 and 5 of induction of anti-ADH RNA (see below), then these results indicate that antisense RNA levels are induced to levels that are 3×, 6× and 3× that of the ADH mRNA in the clones ADHa1, ADHa2 and ADHa3. These ratios of anti-ADH RNA to ADH mRNA are minimum estimates as the tri-molecular hybrids that form between the anti-ADH RNA, the ADH mRNA, and the protection fragment AP1 give rise to diverse protected RNAs that are not readily quantifiable. At most, these structures are present at a level equal to the ADH mRNA, which is the least abundant of these three RNAs. If this is the case then the estimate anti-ADH RNA levels must be increased by an amount equal to the ADH mRNA. This increases the estimate of anti-ADH RNA to 4×, 7×, and 4× that of ADH mRNA in clones ADHa1, ADHa2 and ADHa3 under inducing conditions that inhibit the expression of ADH.

Examination of ADH mRNA and the 5′sense-ADH RNA in the control clones ADHc1 and ADHc2 are shown in figure 3b. The protection fragment in this experiment is SP1 (arrow 1, lane 9), which protects both the ADH mRNA and the 5′sense-ADH RNA. Arrows 3 and 4 indicate the protection fragments of the 5′sense-ADH RNA (see Materials and Methods, the RNase Protection section, for a description of these bands) while arrow 2

Table 1. Quantitation of ADH RNAs in Figures 3, 4, and 6. The indicated bands from the autoradiographs shown in figures 3, and 5 were quantitated, adjusted for loading errors, normalized, and then averaged with duplicate experiments as described in the Materials and Methods section.

clone	Days in Copper	Fig. 3a		Fig. 3b		Fig.4	Fig. 6	
		mRNA	anti-RNA	mRNA	5'sense RNA	mRNA	mRNA	hybrids
ADHa1	0	16.4	11.4			20	24	1
	1		41			33		12
	5		57			24		8
ADHa2	0	15	--			70	100	1.6
	1		90			100		41
	5		90			75		50
ADHa3	0	12	--			38	65	--
	1		29.7			20		6.1
	5		43.2			25		7.2
ADHc1	0			20	13	47		
	1			44	87	72		
	5			41	84	38		
ADHc2	0			2.5	--	7.6		
	1			2.3	5.4	11.5		
	5			2.7	6.9	12.2		

indicates the protection fragment from the ADH mRNA. As in Figure 3a these results have been quantitated and are presented in Table 1.

The tri-molecular structures that form with the ADH mRNA when anti-ADH RNA is present, make accurate analysis of ADH mRNA levels with the protection fragment SP1 impossible when anti-ADH mRNA is induced. However, it is important to know the levels of the ADH mRNA at these time points as it allows us to distinguish between two mechanisms of antisense inhibition of ADH activity. These two mechanisms are that the ADH mRNA is being targeted for degradation, in which case we expect to see a decrease in mRNA levels, or that stable ADH mRNA is being prevented from being translated by some other mechanism. In the latter case we expect no change in the ADH mRNA levels. To determine ADH mRNA levels at all time points we have done an RNase protection experiment using radiolabelled protection fragment SP2 (see figure 1b). As this RNA hybridizes to the ADH mRNA just 3′ to the region targeted by the anti-ADH RNA its binding is not interfered with by the anti-ADH RNA. The results of this experiment are shown in figure 4. Lane 21 shows the probe alone (arrow 1). Lanes 1−15 show the results of hybridizing 5 μl (shown below to contain a mass of protection RNA that is in excess of that required to saturate the ADH mRNA) of the probe to 5 μg of total RNA from each of the clones following either no induction of anti-ADH or 5′sense-ADH RNA, time point 0, or following 1 or 5 days of growth in inducing conditions. Longer exposures show protection in clone ADHc2 lanes (14−16) similar to ADHc1 (not shown). Lane 20 shows the same experiment done with untransformed cells. The appropriate sized protection fragment is about 90 nucleotides long and indicated by arrow #2. This experiment was done twice and RP49 protection used to correct for any loading errors (shown below the lanes). Quantitation of these intensities, as determined by densitometric scanning, is presented in Table 1 and shows that there has been no reduction in ADH mRNA levels when anti-ADH RNA is induced. Thus, we conclude that the mechanism of inhibition of ADH is not the targeting of its RNA for degradation. This finding indicates that the mechanism of ADH inhibition is the prevention of translation of ADH mRNA or some other aspect of RNA maturation or function.

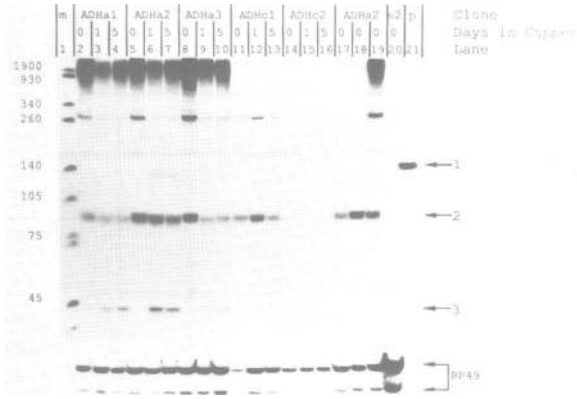

Figure 4. Analysis of ADH mRNA Levels. RNA from each of the 5 clones listed as well as from untransformed S2/M3 (S2) cells was collected before the addition of copper (day 0) or following growth in copper for 1 or 5 days. An RNase protection experiment was done using radiolabelled SP2 (figure 1) as the protection fragment (lane 21, arrow 1). 5 μl of SP2 were used in lanes 2 – 16. Lanes 17 – 19 show the results of protection of RNA from clone ADHa2, day 0, using .1, 1 and 10 μl of SP2. The appropriate protected radiolabelled RNA is indicated by arrow 2. Arrow 3 indicates a protected RNA that is due to regions of homology in the polylinkers that exist in both the transcription vector pRMHa-1 and the vector pGEM4 used to synthesize the SP2 probe. The abbreviations m,p,and s2 stand for molecular weight markers, probe and S2/M3 cells respectively. The results of the protection of RP49 mRNA are shown and used to correct for loading errors.

Lanes 17 – 19 are controls that show the results of protection of 5 μg of the 0 time point from clone ADHa2 using .1, 1 or 10 μl of protection fragment SP2. As there is no significant difference in intensity between protection with 1 μl, 5 μl (lane 4), or 10 μl we conclude that the protection probe is present in saturating amounts when 5 μl is used. Several of the smaller bands seen in lanes 1 – 12 are also seen in the untransformed cells (lane 16) and represent small regions of homology between the probe and other RNAs. One lower molecular weight band (arrow 3) is inducible and present only in the transformed cells. This is due to a small (30 base) region of the polylinker in the vector used to synthesize the riboprobe that is homologous with the polylinker in the expression vector used to express the anti-ADH and 5′sense-ADH RNAs. Above the appropriately sized protection fragment there are some minor bands and a large smear at the top of the gel that is larger than the probe itself. Examining lanes 13 – 15 we note that this smear is present only at high probe concentrations. We presume that it is due to breakdown products of the radiolabelled probe binding, when present at high concentrations, to some DNA that was not completely degraded. We do not understand the origins of the other bands that are larger than the probe itself. However, they do not confuse the issue as they are relatively minor in abundance and cannot be due to ADH mRNA hybridizing with the probe.

Examination of Hybrid RNA

We have done two experiments to examine first whether hybrids are forming between the ADH mRNA and the anti-ADH RNA, and then to examine the fate of these hybrids. The first experiment qualitatively examines the nature of the hybrids that are formed in cells. The hybrids formed between ADH preRNA or ADH mRNA and the anti-ADH RNA and the sizes of the resulting RNase protection fragments are diagrammed in figure 5a. In figure 5b we show the protected RNA obtained from the 5 clones when their RNA

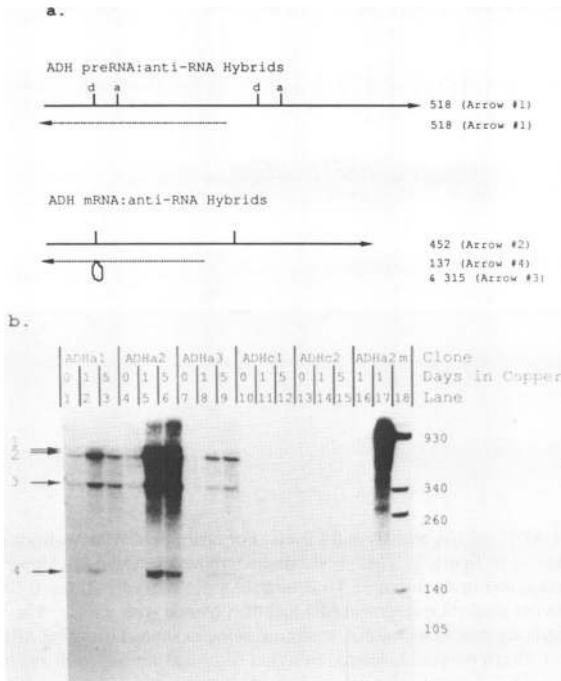

Figure 5. *In Vivo* Hybrids. *a.* The hybrid formed between the ADH preRNA and anti-ADH RNA is shown on top. The antisense RNA is represented by a dotted line. The splice donor (d) and acceptor (a) sites for the two introns are shown. Below this is shown the hybrids formed between the anti-ADH RNA and the ADH mRNA. The vertical lines on the mRNA indicate the positions of the removed introns. As the antisense RNA was derived from genomic sequences, those sequences complementary to intron sequences will be 'looped out' in the hybrid and susceptible to RNase cleavage. To the right of each RNA is shown the expected size of the RNA fragment(s) following digestion of the hybrid with RNase. In parentheses is given the arrow # that each fragment is indicated with in Figure 5b. *b.* RNAs collected from the indicated clones that had been grown for the indicated number of days in copper were collected and treated with RNase T1. This was done without the addition of protection RNA and without a hybridization step. The protected RNAs were electrophoresed, transferred to a nylon filter and probed with radiolabelled DS1. Lanes 16 and 17 show RNA from clone ADHa2, day 1, that had been either denatured in 80% formamide 85°C and immediately treated with RNase (lane 16) or had not been treated with RNase. The arrows indicate the 4 protected RNAs that were predicted in figure 5a. The abbreviation m stands for molecular weight markers.

was extracted and treated with RNase T1 without *in vitro* hybridization. A reconstruction experiment (data not shown) shows that hybrids are not forming during our RNA extraction procedures so that any protected fragments we observe exist as hybrids in the cell.

Radiolabelled DS1 (see Figure 1b) was used to probe the protected RNAs that had been transferred to a nylon filter in Figure 5b. This double stranded probe should detect all of the possible protected fragments. Indeed, we see the protection of all four of the expected bands. The identity of these four bands has been confirmed by using region and strand-specific probes from within this region (not shown). The only exception to the diagram in 5a is that a small amount of the 315 bp fragment is derived from the mRNA as it hybridizes to radiolabelled SP1. This would be expected if there was digestion of ADH

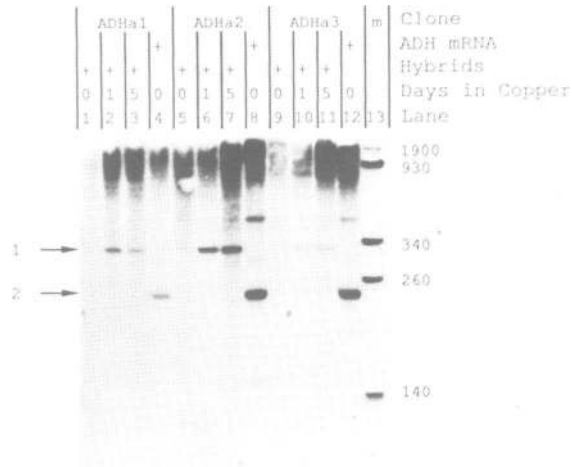

Figure 6. Comparison of ADH mRNA and Hybrid Levels. For analysis of ADH hybrids (lanes 1−3, 5−7 and 9−11) RNAs were treated as in figure 5. The '+'s' one line above the Days in Copper line indicates that *in vivo* hybrids are being examined in these lanes. To determine mRNA levels at day 0 (lanes 4, 8 and 12) the RNA was hybridized with the protection fragment SP1 and then treated with RNase. The '+'s' two lines above the Days in Copper line indicate that ADH mRNA levels are being examined using the SP1 protection fragment. The protected RNAs were electrophoresed, blotted to nylon filter and probed with radiolabelled AP2. Arrow #1 indicates the protected RNA derived from *in vivo* hybrids (fragment #3 in figure 5a). Arrow #2 indicates the expected RNA fragment derived from protection of ADH mRNA by SP1. The abbreviation m stands for molecular weight markers.

mRNA opposite to the looped out intron in the mRNA-anti RNA hybrid. It would also be generated if the 137 bp hybrid region is not totally stable. This is quite likely as the 137 fragment appears to be less intense than the 315 and it should be of equal intensity.

Figure 5 demonstrates that inducible hybrids are forming between the anti-ADH and the ADH preRNA and ADH mRNA. We see that the hybrids are predominantly forming with the mRNA. This experiment does not give an indication of the amounts of hybrid relative to the ADH mRNA. This amount was estimated from the experiment shown in figure 6. Here we determine the amount of ADH mRNA that is present by protection of RNA from uninduced cells with the probe SP1 (lanes 4, 8 and 12). As the ADH levels do not change upon induction of anti-ADH RNA this also represents the levels of ADH mRNA present after induction of the anti-ADH RNA in these three clones. To obtain estimates of the levels of hybrid RNA under conditions of no induction of anti-ADH RNA or following induction for 1 or 5 days, total RNA from these time points was treated with RNase without prior *in vitro* hybridization (lanes 1−3,5−7, and 9−11). The protected RNAs were electrophoresed and blotted to a nylon filter. This blot was probed with radiolabelled AP2. This probe bears the same amount of homology to one strand of the protected *in vivo* hybrid (arrow 1) as to the hybrid formed between the ADH mRNA and SP1 *in vitro* (arrow 2 in lanes 4, 8, and 12). We can therefore compare the levels of each. A previous experiment showed that our protection of ADH mRNA is close to 100% efficient under these conditions (not shown).

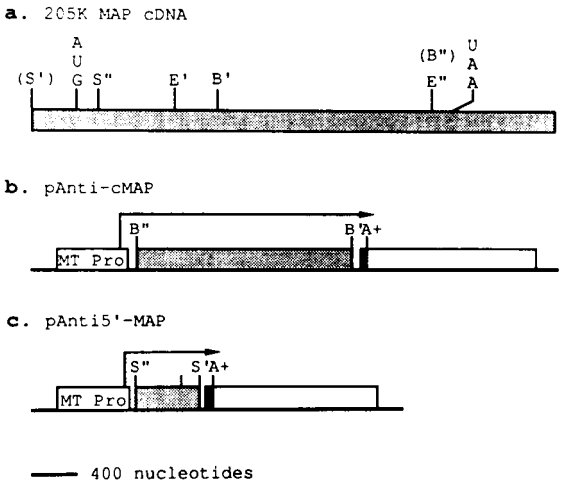

Figure 7. Anti-MAP Plasmids. *a.* The 205K MAP cDNA used for the construction of the anti-MAP genes extends from 400 bases 5′ to the start of translation (AUG) to 1 kb 3′ of the putative end of translation (UAA). The two *Eco*RI sites (E′ and E″), *Bam*HI sites (B′ and B″) and the two *Sal*I sites (S′ and S″) used in constructing the anti-MAP genes are shown. The 5′ *Sal*I site (S′) does not exit in the cDNA but is found in the plasmid that the cDNA was cloned into. The 3′ *Bam*HI site (B″) also does not exist in the cDNA but is derived from a plasmid that the *Eco*RI fragment was cloned into. *b.* pAnti-cMAP contains the 2.1 kb *Bam*HI fragment cloned in reverse orientation into the transcription vector pRmHa-1. The filled rectangle represents, as in figure 1, ADH sequences that contain the polyadenylation signal (A^+). The unlabelled open boxes are, again, genomic sequences that are 3′ of the ADH polyadenylation signal. *c.* pAnti-5′MAP is similar to pAnti-cMAP except that it contains the *Sal*I fragment containing 477 bp of 5′ untranslated sequence and the first 165 bp of translated sequence from the 205K MAP gene. These have been cloned in the reverse orientation with respect to the metallothionein promoter.

By comparing the intensity of the 315 nucleotide band (arrow 1) with that at 240 (arrow 2) we see that hybrid does indeed account for much of the ADH mRNA. Quantitation is difficult here as we can not assay the hybrid of an unrelated RNA in the lanes that examine *in vivo* hybrid levels. This prevents adjustment for loading errors or losses during manipulation of the RNA. Manipulation and loading errors in previous experiments have led to correction factors between 1 and 3. As with the other gels this experiment was done twice and the results quantitated in Table 1.

Anti-205K MAP Genes

In an attempt to reduce the levels of 205K MAP we have constructed two anti-MAP genes whose transcription are driven by the metallothionein promoter. These are shown in figure 7. Figure 7a shows the general structure of the 205K MAP cDNA. The precise locations of the 5′ and 3′ ends have not been determined, but the 5′ end certainly extends beyond the extent of the cDNA shown here (Goldstein and Irminger-Finger, unpublished). The 5′ *Sal*I site, denoted S′ is derived from the polylinker that the MAP cDNA was cloned into. A large intron exists between the two *Eco*RI sites (E′ and E″) in the genomic DNA. The AUG start of translation codon and UAA stop codon are based on sequence data (Goldstein, Laymon and Irminger-Finger, unpublished).

Figure 7b shows pAnti-cMAP that contains the 2.1 kb *Bam*HI fragment cloned in the reverse orientation with respect to the metallothionein promoter. Figure 7c shows pAnti-5′

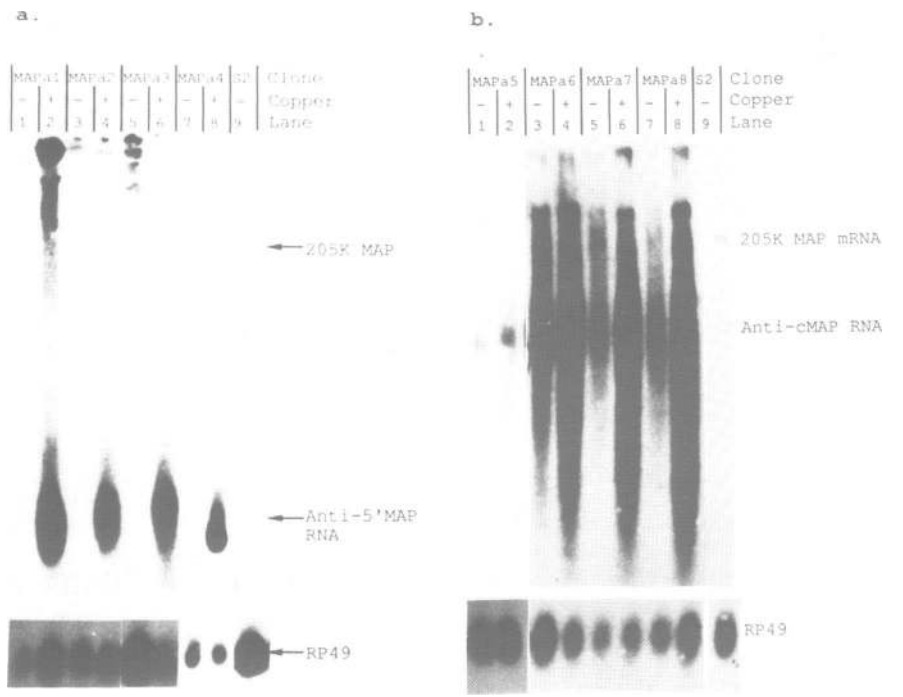

Figure 8. Analysis of 205K MAP RNA Levels. *a.* Poly A^+ RNA was isolated from the clones MAPa1, MAPa2, MAPa3 and MAPa4 either before the induction of anti-5'MAP genes (−) or following their induction by growth of the cells for 18 hours in 0.3 mM $CuSO_4$ (+). Poly A^+ RNA was also isolated from untransformed S2/M3 (S2) cells lane 9. This RNA was electrophoresed on formaldehyde/agarose gels, blotted to GeneScreen nylon membrane and probed with radiolabelled probe that will hybridize to both the anti-5'MAP RNA and 205K MAP mRNA. In this exposure 205K MAP mRNA is not visible in the overloaded lane 9. In longer exposures it is detctable. Beneath the lanes are shown the reprobing of the blot for RP49 mRNA. *b.* A similar analysis of poly A^+ RNA isolated from the anti-cMAP containing clones MAPa5, MAPa6, MAPa7 and MAPa8 is shown. Lane 9 shows poly A^+ RNA from S2/M3 cells (S2). Arrow 1 indicates the 205K MAP mRNA. Arrow 2 indicates the correct size of anti-cMAP. Reprobing of this blot for RP49 mRNA is shown.

MAP, which contains the 600 bp *SalI* fragment containing 477 bp of 5′ untranslated sequences and 165 bp of translated sequences. These plasmids were transformed into cells and clones were obtained that contain copies of either pAnti-cMAP or pAnti-5′ MAP.

Analysis of RNA from Anti-MAP Clones

Figure 8 shows an analysis of the 205K MAP poly (A+) RNAs from 4 clones containing anti-5′ MAP, 4 clones containing anti-cMAP and untransformed S2/M3 cells. RNA from clones MAPa1, MAPa2, MAPa3 and MAPa4, which contain anti-5′ MAP genes, was analyzed by electrophoresis in agarose/formaldehyde gels followed by Northern blotting of RNA to GeneScreen and probing for MAP RNA (figure 8a). In all four clones we see a dramatic induction of anti-5′ MAP RNA levels that vastly exceed the levels of MAP mRNA, which is not detectable, in this exposure, in the overloaded lane 9, containing RNA from untransformed cells. In longer exposures 205K MAP mRNA is detectable (not shown). The results of reprobing this blot for RP49 mRNA are shown beneath each lane.

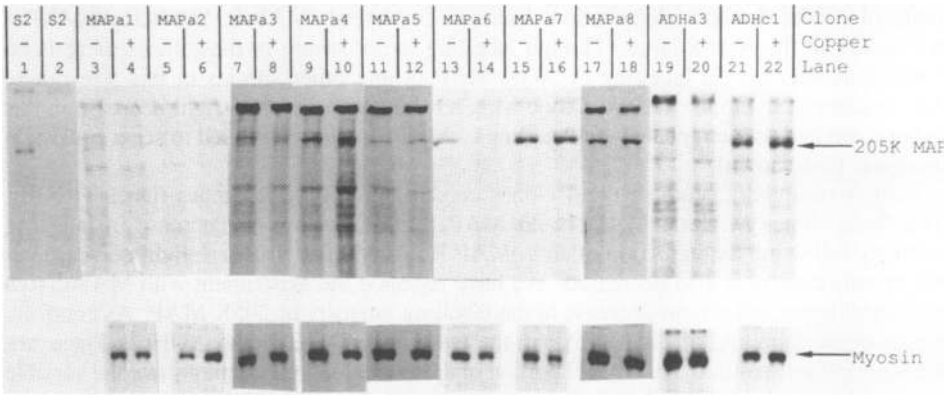

Figure 9. Immunoprecipitation of Newly Synthesized 205K MAP. The indicated clones were grown for 14–16 hours in the presence(+) or absence (−) of 0.3 mM $CuSO_4$ and then metabolically labelled with ^{35}S-methionine for 6 hours in the presence or absence of 0.3 mM $CuSO_4$. Following this labelling, cell extracts were prepared and 205K MAP was immunoprecipitated. These samples were electrophoresed on SDS-PAGE gels, which were then dried and exposed to x-ray film. Lane 1 shows precipitation with preimmune serum and lane 2 shows precipitation of 205K MAP from untransformed S2/M3 cells (S2). Immunoprecipitation of cytoplasmic myosin heavy chain was also done and used to correct for any labelling differences that might exist between untreated cells and those grown in 0.3 mM $CuSO_4$.

A similar analysis of RNA from the clones which bear anti-cMAP genes is shown in 8b. Again RNA from S2/M3 cells is shown for comparison. In this lane 205K MAP mRNA can be detected. Anti-5′ MAP RNA of the appropriate size is labelled. We often detect transcripts larger than the appropriate size due to the polyadenylation signal functioning at less than 100% efficiency or to disrupted genes (27). The signal below the appropriate size probably indicates that this particular RNA is unstable in the cell. Reprobing of this blot with a probe that hybridizes to RP49 mRNA shows that the loadings are approximately the same in all of the lanes. These results then indicate that the anti-MAP RNA, though not perfectly intact, exists in vast excess over MAP mRNA.

Analysis of 205K MAP Synthesis Rates

To determine if the presence of anti-MAP RNA was preventing the translation of MAP mRNA we initially analyzed 205K MAP levels by Western analysis of total cellular proteins using an antibody that recognizes 205K MAP. This did not indicate any reductions in 205K MAP levels after 5 days of growth in copper-containing media (not shown). These cell lines also did not show a significant reduction in growth rate when anti-MAP RNA was induced (not shown). A more sensitive assay of translation of 205K MAP mRNA is to measure newly synthesized 205K MAP before or after the induction of anti-MAP RNA. Therefore, we treated cells with 3 mM $CuSO_4$ for 18 hours and then metabolically labelled them with ^{35}S-methionine for 6 hours. Cells were also grown and labelled in the absence of $CuSO_4$. Following labelling, cell extract was prepared and 205K MAP was immunoprecipitated using an antibody against 205K MAP. We also immunoprecipitated cytoplasmic myosin which serves as a control for any differences in labelling.

The results of these immunoprecipitations are shown in figure 9. In the first lane we see the 205K MAP precipitated from S2/M3 cells. Lane 2 shows immunoprecipitation when preimmune serum was used. Minor bands are observed but there are none in the

range of 205 kd. Immunoprecipitations from clones MAPa1, MAPa2, MAPa3 and MAPa4 are shown in the next 8 lanes. Though labelling is not strong in these lanes there is no observable decrease in labelling of 205K MAP or any other species in this size range. This is clearest in clone MAPa4. Clone MAPa3 showed a possible slight decrease in this experiment and so we repeated the labelling of MAPa3 twice and failed to see a consistent decrease (not shown).

Similar results are seen for the 4 clones containing anti-cMAP genes (lanes 11−18). The three clones MAPa5, MAPa7 and MAPa8 clearly show no decrease in labelling intensity following the induction of anti-cMAP RNA. MAPa6 shows a slight decrease but the myosin control is also decreased. We have repeated the experiment with MAPa6 two additional times and see no decrease in the labelling intensity of 205K MAP. As controls, we show the labelling of 205K MAP in the two clones ADHa3 and ADHc1. These are the same clones analyzed in the ADH portion of this paper, and they demonstrate the variable level of labelling of 205K MAP that we observe in these experiments.

These results and the RNA analysis indicate that a large excess of either of these two antisense 205K MAP RNAs is not capable of inhibiting the translation of 205K MAP mRNA.

DISCUSSION

The results of the experiments presented here indicate that antisense genes utilizing a *Drosophila melanogaster* metallothionein promoter can inducibly inhibit gene expression in cultured *Drosophila* cell lines. This has been demonstrated by the inhibition of ADH activity by 75→90% in cell lines containing anti-ADH genes. This is an important point as it allows *Drosophila* biologists to create dominant, conditional amorphic or hypomorphic mutations in cultured cells. Examination of the phenotypes of such mutations will be useful in determining the function(s) of various gene products being studied in the cultured *Drosophila* cells. Certain genes may not be amenable to this approach as even a reduction of >90% of the levels of some gene products does not lead to a noticeable phenotype (41). However, there are certainly cases where hypomorphic mutations will result in an observable phenotype. The results of attempts to inhibit the expression of 205K MAP demonstrate that not all such antisense genes will be successful in inhibiting gene expression. Our examination into the fate of hybrid RNAs that form between ADH mRNA and antisense RNA address questions about the cellular response to the presence of hybrid RNAs.

We have examined the mechanism of inhibition of ADH expression at the RNA level. ADH mRNA levels, assayed in figure 4, show no change during inhibition but rather a large portion of the mRNA is found hybridized with the anti-ADH RNA. This result allows us to conclude that the ADH mRNA is not being targeted for degradation by the presence of antisense RNA or hybrids as has been seen in a variety of other systems where antisense genes have been employed. This result is different from the results, in cultured *Drosophila* cells, of experiments that used antisense genes under the control of the promoter from the 70 kd heat-shock protein (HSP70) to reduce expression of the HSP26 gene. In this case HSP26 mRNA levels were reduced by the presence of antisense RNA (9). We do not have an explanation for the difference in these results. Potential reasons include different effects on the stability of the hybrid RNAs due to the formation, or disruption, of secondary structures within the RNAs; special properties of HSP mRNAs that make their metabolism different than other RNAs; or special properties of the chimeric ADH mRNA. Whatever the reasons for these different observations, they indicate that the destabilization of the

target mRNA is not necessarily a unique indicator of the presence of functional antisense genes.

Examining the hybrids that form between the anti-ADH and ADH sense RNA we have noted that the hybrids form primarily between the anti-ADH RNA and the properly spliced ADH mRNA. This indicates that the mechanism of antisense inhibition of expression is not by binding to pre-mRNA in the nucleus and preventing splicing even though the antisense RNA covers the entire first intron. We do note, at a much lower level, hybrids between the anti-ADH RNA and unspliced ADH pre-mRNA. Detection of hybrids with ADH pre-mRNA, which are presumably in the nucleus, is not entirely surprising as nuclear hybrids have been detected in another antisense experiment in mammalian cells (7). Thus, the simplest explanation concerning the mechanism of action of the anti-ADH RNA is that it hybridizes to the properly spliced ADH mRNA in the nucleus or the cytoplasm and prevents transport from the nucleus or translational initiation due to the fact that the hybrid region includes 40 nucleotides of the 5′ untranslated sequences and the start of translation AUG. As the hybrid region also contains 316 nucleotides of translated RNA, inhibition of translational elongation could also be a factor.

The inhibition of ADH expression and formation of hybrids is achieved with anti-ADH RNA levels that are present in a 4−7 fold excess over the ADH mRNA levels (figure 3a and Table 1). This ratio of antisense:sense RNA is similar to the ratio that was required to reduce HSP26 expression in cultured *Drosophila* cells (42) and to the levels required for inhibition in experiments in various other systems (2,6,9,14,15). This level is much lower than the 50−200 fold excess required in several other antisense experiments in other systems (5,6,13). We do not understand the reasons for these differences.

In contrast to our success in inhibiting ADH expression, our attempts to reduce the expression of 205K MAP have been unsuccessful. At present we do not understand the reason for this. Anti-MAP RNA, in the clones examined, is in vast excess over the 205K MAP mRNA (figure 8) but newly synthesized 205K MAP is not reduced by the induction of anti-MAP RNA (figure 9). These observations are true for two anti-MAP genes that synthesize RNA that should hybridize to either the 5′ region of 205K MAP mRNA, including 5′ untranslated sequences and the first 165 translated nucleotides, or that should hybridize to 2.1 kb of translated sequences in the mRNA.

Possible explanations for our failure to inhibit 205K MAP expression include the existence of secondary structure within the 205K MAP mRNA that prevents hybrid formation or the presence of proteins bound to the mRNA making it inaccessible to antisense RNA. Results from Sue Lindquist's laboratory suggest that antisense genes which target different regions of the HSP70 mRNA vary in their effectiveness (42). Similar results have also been seen in other systems (6,13). Perhaps different anti-MAP genes directed against different regions of the 205K MAP mRNA will prove successful.

Another possible explaination of the difference in our ability to inhibit the expression of these two genes lies in the fact that the ADH genes were exogenously added by cotransfection with the antisense genes while the 205K MAP gene is an endogenous gene. Most of the ADH genes will be located in the large arrays that form during transformation in this system. The antisense ADH genes are also located in these arrays and are therefore in close proximity to the ADH genes that they are inhibiting. In the case of 205K MAP, it is likely that the transfected antisense MAP genes are located in large arrays whose chromosomal locations are not adjacent to the endogenous 205K MAP gene. It is possible then, that the ADH mRNA experiences a high local concentration of anti-ADH RNA and

that this is necessary for inhibition. The 205K MAP mRNA may never encounter an equally high concentration of antisense RNA.

Prior to this study the only other inducible promoter used in cultured *Drosophila* cells for antisense experiments was the HSP70 promoter. The HSP70 promoter is a strong, highly inducible promoter that is well suited for antisense genes that target HSP mRNAs, which are induced at the same time as the antisense RNA. As the HSP70 promoter is down regulated after long periods of heat-shock (43), it may not be ideal for experiments that require the presence of high levels of antisense RNA for a period of several days in order to obtain a reduction in the levels of a protein that is produced constitutively. The metallothionein promoter used in these experiments is perhaps more well suited to inhibition of a constitutively produced protein as this promoter avoids this problem.

The results with 205K MAP indicate that there are still factors, which we do not yet understand, that influence the success of antisense genes to inhibit gene expression. However, our results with ADH suggest that antisense genes based on the metallothionein promoter will be quite useful to *Drosophila* biologists by allowing the construction of dominant, inducible hypomorphic or amorphic mutations in cultured cells.

ACKNOWLEDGEMENTS

We thank Drs. Peter Cherbas, Lucy Cherbas, Sue Lindquist and Dan Kiehart for their useful comments on the manuscript.

This work was supported by NIH grants GM35252 and GM29301.

*To whom correspondence should be addressed

+Present address: University of Arizona, Department of Molecular and Cellular Biology, Biosciences West Building, Tucson, AZ 85721, USA

REFERENCES

1. Coleman, J., P. Green, and M. Inouye. 1984. The use of RNAs complementary to specific mRNAs to regulate the expression of individual bacterial genes. Cell **37**:429–436.
2. Crowley, T.E., W. Nellen, R.H. Gomer, and R.A. Firtel. 1985. Phenocopy of discoidin I-minus mutants by antisense transformation in *Dictylostelium*. Cell **43**:633–641.
3. Ecker, J.R., and R.W. Davis. 1986. Inhibition of gene expression in plant cells by expression of antisense RNA. PNAS **83**:5372–5376.
4. Giebelhaus, D.H., D.W. Eib, and R.T. Moon. 1988. Antisense RNA inhibits expression of membrane skeleton protein 4.1 during embryonic development of *Xenopus*. Cell **53**:601–615.
5. Izant, J.G., and H. Weintraub. 1984. Inhibition of thymidine kinase gene expression by anti-sense RNA: a molecular approach to genetic analysis. Cell **36**:1007–1015.
6. Izant, J.G., and H. Weintraub. 1985. Constitutive and conditional suppression of exogenous and endogenous genes by anti-sense RNA. Science **229**:345–352.
7. Kim, S., and B.J. Wold. 1985. Stable reduction of thymidine kinase activity in cells expressing high levels of anti-sense RNA. Cell **42**:129–138.
8. Knecht, D.A., and W.F. Loomis. 1987. Antisense RNA inactivation of myosin heavy chain gene expression in *Dictyostelium discoideum*. Science **236**:1081–1091.
9. McGarry, T.J., and S. Lindquist. 1986. Inhibition of heat shock protein synthesis by heat-inducible antisense RNA. PNAS **83**:399–403.
10. Strickland, S., J. Huarte, D. Belin, A. Vassalli, R.J. Rickles, J.-D Vassalli. 1988. Antisense RNA directed against the 3′ noncoding region prevents dormant mRNA activation in mouse oocytes. Science **241**:680–684.
11. Xiao, W. and G.H. Rank. 1988. Generation of an *ilv* bradytrophic phenocopy in yeast by antisense RNA. Curr. Genet. **13**:283–289.

12. Rosenberg, U.B., A. Preiss, E. Seifert, H. Jackle, and D.C. Knipple. 1985. Production of phenocopies by *Kruppel* antisense RNA injection into *Drosophila* embryos. Nature **313**:703–706.
13. Melton, D.A. 1985. Injected anti-sense RNAs specifically block messenger RNA translation *in vivo*. PNAS **82**:144–148.
14. Pecorino, L.T., R.J. Rickles, and S. Strickland. 1988. Anti-sense inhibition of tissue plasminogen activator production in differentiated F9 teratocarcinoma cells. Developmental Biology **129**:408–416.
15. Rothstein, S.J., J. DiNaio, M. Strand, and D. Rice. 1987. Stable and heritable inhibition of the expression of nopaline synthase in tobacco expressing antisense RNA. Proc. Natl. Acad. Sci. USA **84**:8439–8443.
16. Delauney, A.J., Z. Tabaeizadeh, and D.P.S. Verma. 1988. A stable bifunctional antisense transcript inhibiting gene expression in transgenic plants. PNAS **85**:4300–4304.
17. Smith, C.J.S., C.D. Watson, J. Ray, C.R. Bird, P.C. Morris, W. Schuch, and D. Grierson. 1988. Antisense RNA inhibition of polygalacturonase gene expression in transgenic tomatoes. Nature **334**:724–726.
18. Bass, B.L., and H. Weintraub. 1987. A developmentally regulated activity that unwinds RNA duplexes. Cell **48**:607–613.
19. Rebagliati, M.R., and D.A. Melton. 1987. Antisense RNA injections in fertilized frog eggs reveal an RNA duplex unwinding activity. Cell **48**:599–605.
20. Harland, R., and H. Weintraub. 1985. Translation of mRNA injected into *Xenopus* Oocytes is specifically inhibited by antisense RNA. JCB **101**:1094–1099.
21. Melton, D.A., P.A. Krieg, M.R. Rebagliati, T. Maniatis, K. Zinn, and M.R. Green. 1984. Efficient *in vitro* synthesis of biologically active RNA and RNA hybridization probes from plasmids containing a bacteriophage SP6 promoter. Nucleic Acids Research **12**:7035–7056.
22. Wormington, W.M. 1986. Stable repression of ribosomal protein L1 synthesis in *Xenopus* oocytes by microinjection of antisense RNA. PNAS **83**:8639–8643.
23. Goldstein, L.S.B., R.A. Laymon, and J.R. McIntosh. 1986. A microtubule-associated protein in *Drosophila melanogaster*. Identification, characterization, and isolation of coding sequences. JCB **102**:2076–2087.
24. Schneider, I. 1972. Cell lines derived from late embryonic stages of *Drosophila melanogaster*. J. Embryol. exp. Morph. **27**:353–365.
25. Lindquist, S.L., S. Sonoda, T. Cox, and K. Slusser. 1982. Instant medium for *Drosophila* tissue culture cells. *Drosophila* Information Service **58**:163–164.
26. Wigler, M., A. Pellicer, S. Silverstein, R. Axel, G. Urlaub, and L Chasin. 1979. DNA-mediated transfer of the adenine phosphoribosyltransferase locus into mammalian cells. PNAS **76**:1373–1376.
27. Bunch, T.A., Y. Grinblat, and L.S.B. Goldstein. 1988. Characterization and use of the *Drosophila* metallothionein promoter in cultured *Drosophila melanogaster* cells. Nucleic Acids Research **16**:1043–1061.
28. Bourouis, M., and B. Jarry. 1983. Vectors containing a prokaryotic dihydrofolate reductase gene transform *Drosophila* cells to methotrexate-resistance. EMBO J. **2**:1099–1104.
29. Moss, R.E. 1985. Analysis of a transformation system for *Drosophila* tissue culture cells. Ph.D. Thesis. Harvard University.
30. Kiehart, D.P. and R. Feghali. 1986. Cytoplasmic Myosin from *Drosophila melanogaster*. JCB **103**:1517–1525.
31. Laemmli, U.K. 1970. Cleavage of structural proteins during the assembly of the head of bacteriophage T4. Nature **227**:680–685.
32. Cherbas, L., R.A. Schulz, M.M.D. Koehler, C. Savakis, and P. Cherbas. 1986. Structure of the *EIP28/29* gene, an ecdysone-inducible gene from *Drosophila*. J. Mol. Biol. **189**:617–631.
33. Goldberg, D.A. 1980. Isolation and partial characterization of the *Drosophila* alcohol dehydrogenase gene. PNAS **77**:5794–5798.
34. Feinberg, A.P., and B. Vogelstein. 1983. A technique for radiolabeling DNA restriction endonuclease fragments to high specific activity. Analytical Biochemistry **132**:6–13.
35. Yanisch-Perron, C., J. Vieira, and J. Messing. 1985. Improved M13 phage cloning vectors and host strains: nucleotide sequences of the M13mp18 and pUC19 vectors. Gene **33**:103–119.
36. O'Connell, P. and M. Rosbash. 1984. Sequence, structure, and codon preference of the *Drosophila* ribosomal protein 49 gene. Nucleic Acids Research **12**:5495–5513.
37. Maniatis, T., E.F. Fritsch, and J. Sambrook. 1982. Molecular Cloning: A Laboratory Manual. Cold Spring Harbor Laboratory, Cold Spring Harbor, New York.
38. Church, G., and W. Gilbert. 1984. Genomic sequencing. PNAS **81**:1991–1995.
39. Denhardt, D.T. 1966. A membrane-filter technique for the detection of complementary DNA. Bioch. Bioph. Res. Com. **23**:641–652.
40. Sofer, W., and H. Ursprung. 1968. *Drosophila* alcohol dehydrogenase. Purification and partial characterization. J. Biol. Chem. **243**:3110–3115.

41. Gelbart, W., M. McCarron, and A. Chovnick. 1976. Extension of the limits of the XDH structural element in *Drosophila melanogaster*. Genetics **84**:211–232.
42. Lindquist, S., T.J. McGarry, and K. Golic. 1988. Use of antisense RNA in studies of the heat-shock response, p. 71–77. *In* Melton, D.A. (ed.), Current Communications in Molecular Biology: Antisense RNA and DNA. Cold Spring Harbor Laboratory, Cold Spring Harbor, New York.
43. Lindquist, S. 1980. Varying patterns of protein synthesis on *Drosophila* during heat shock: implications for regulation. Dev.Biol. **77**:463–479.

This article, submitted on disc, has been automatically converted into this typeset format by the publisher.